


The Cytochrome P450 2C8*3 Variant (rs11572080) Is Associated with Improved Asthma Symptom Control in Children and Altered Lipid Mediator Production and Inflammatory Response in Human Bronchial Epithelial Cells[□]

Marysol Almestica-Roberts, Nam D. Nguyen, Lili Sun, Samantha N. Serna, Emmanuel Rapp, Katherine L. Burrell-Gerbers, Tosifa A. Memon, Bryan L. Stone, Flory L. Nkoy, John G. Lamb, Cassandra E. Deering-Rice, Joseph E. Rower, and  Christopher A. Reilly

Department of Pharmacology and Toxicology, Center for Human Toxicology (M.A.-R., N.D.N., L.S., S.N.S., E.R., K.L.B.-G., T.A.M., J.G.L., C.E.D.-R., J.E.R., C.A.R.) and Department of Pediatrics, School of Medicine (B.L.S., F.L.N.), University of Utah, Salt Lake City, Utah

Received February 3, 2024; accepted May 14, 2024

ABSTRACT

This study investigated an association between the cytochrome P450 (CYP) 2C8*3 polymorphism with asthma symptom control in children and changes in lipid metabolism and pro-inflammatory signaling by human bronchial epithelial cells (HBECs) treated with cigarette smoke condensate (CSC). CYP genes are inherently variable in sequence, and while such variations are known to produce clinically relevant effects on drug pharmacokinetics and pharmacodynamics, the effects on endogenous substrate metabolism and associated physiologic processes are less understood. In this study, CYP2C8*3 was associated with improved asthma symptom control among children: Mean asthma control scores were 3.68 ($n = 207$) for patients with one or more copies of the CYP2C8*3 allele versus 4.42 ($n = 965$) for CYP2C8*1/*1 ($P = 0.0133$). In vitro, CYP2C8*3 was associated with an increase in montelukast 36-hydroxylation and a decrease in linoleic acid metabolism despite lower mRNA and protein expression. Additionally, CYP2C8*3 was associated

with reduced mRNA expression of interleukin-6 (IL-6) and C-X-C motif chemokine ligand 8 (CXCL-8) by HBECs in response to CSC, which was replicated using the soluble epoxide hydrolase inhibitor, 12-[[[tricyclo[3.3.1.1^{3,7}]dec-1-ylamino]carbonyl]amino]-dodecanoic acid. Interestingly, 9(10)- and 12(13)-dihydroxyoctadecenoic acid, the hydrolyzed metabolites of 9(10)- and 12(13)-epoxyoctadecenoic acid, increased the expression of IL-6 and CXCL-8 mRNA by HBECs. This study reveals previously undocumented effects of the CYP2C8*3 variant on the response of HBECs to exogenous stimuli.

SIGNIFICANCE STATEMENT

These findings suggest a role for CYP2C8 in regulating the epoxyoctadecenoic acid:dihydroxyoctadecenoic acid ratio leading to a change in cellular inflammatory responses elicited by environmental stimuli that exacerbate asthma.

Introduction

Asthma causes intermittent narrowing of the airways and increased airway hyperresponsiveness (AHR) (<https://foundation.chestnet.org/patient-education-resources/asthma/>). AHR, defined by an exaggerated

This work was supported by a grant and diversity supplement from National Institutes of Health National Institute of General Medical Sciences [Grant GM121648] and a grant from the National Institute of Environmental Health Sciences [Grant ES017431].

The authors declare no potential conflicts of interest with respect to the research, authorship, and/or publication of this article.

dx.doi.org/10.1124/dmd.124.001684.

[□] This article has supplemental material available at dmd.aspetjournals.org.

response of the airway to pharmacological, physical, and chemical stimuli, is associated with an increased risk of acute asthma exacerbation. Recurrent exacerbations among individuals with asthma are indicative of a progressive worsening of symptom control and a decline in pulmonary function (Meurs et al., 2008; Chapman and Irvin, 2015). According to the 2021 Global Strategy for Asthma Management and Prevention, asthma is a heterogeneous disease defined by variable and recurring respiratory symptoms (i.e., wheeze, shortness of breath, chest tightness or pain, cough) and variable expiratory airflow limitation (<https://ginasthma.org/gina-reports/>). In addition to marked variability in disease pathogenesis, asthma is characterized by variability in therapeutic responses due to complex interactions of genetic and environmental factors (Huo and Zhang, 2018).

Variability in therapeutic responses can arise from genetic polymorphisms in the CYP enzymes. Several CYP enzymes are involved in the

ABBREVIATIONS: AA, arachidonic acid; AHR, airway hyperresponsiveness; AUDA, 12-[[[tricyclo[3.3.1.1^{3,7}]dec-1-ylamino]carbonyl]amino]-dodecanoic acid; BEAS-2B, human bronchial epithelial cell; CSC, cigarette smoke condensate; CXCL-8, C-X-C motif chemokine ligand 8; CYP, cytochrome P450; DiHOME, dihydroxyoctadecenoic acid; EET, epoxyeicosatrienoic acid; EpOME, epoxyoctadecenoic acid; HBEC, human bronchial epithelial cell; HBEC3-KT, normal human bronchial epithelial cells immortalized with CDK4 and hTERT; IL-6, interleukin 6; LA, linoleic acid; LHC-9, Lechner and LaVeck media; ORF, open reading frame; PCR, polymerase chain reaction; PUFA, polyunsaturated fatty acid; SAEC, small airway epithelial cell; sEH, soluble epoxide hydrolase; SNP, single nucleotide polymorphism; UPLC-MS/MS, ultra-performance liquid chromatography-tandem mass spectrometry.

metabolic clearance of asthma therapeutics including CYP3A4 and 3A5, which metabolize inhaled corticosteroids such as fluticasone propionate, budesonide, and beclomethasone dipropionate, as well as salmeterol, a long-acting β_2 -adrenergic receptor agonist (Cazzola et al., 2002; Roberts et al., 2013; Stockmann et al., 2013). In conjunction with cytochrome P450 (CYP)2C8 (major) and CYP2C9 (minor), CYP3A4 and 3A5 also metabolize the cysteinyl leukotriene receptor 1 antagonist montelukast (Karonen et al., 2012; Cardoso et al., 2015). Prior candidate gene studies reported significant associations between nonsynonymous single nucleotide polymorphisms (SNPs) in CYP3A4 (CYP3A4*22) and CYP3A5 (CYP3A5*3) and improved asthma symptom control among children treated with fluticasone propionate and beclomethasone dipropionate, respectively (Stockmann et al., 2013, 2015). A basis for these associations was hypothesized to be reduced hepatic, intestinal, and/or pulmonary expression and activity of the variant enzymes, leading to reduced metabolic clearance of the active drugs (Wang et al., 2011; Arbitrio et al., 2022). Similarly, CYP2C8*3 has been associated with reduced area under the plasma concentration-time curve for montelukast, indicative of increased drug clearance (Hirvensalo et al., 2018).

In addition to xenobiotic metabolism, CYP enzymes are one of three primary enzymatic systems (i.e., cyclooxygenase, lipoxygenase, and CYP) that metabolize the ω -6 and ω -3 polyunsaturated fatty acids (PUFAs) (Bishop-Bailey et al., 2014). Lipid-metabolizing CYPs possess epoxygenase, lipoxygenase-like, and/or ω -hydroxylase enzyme activity. Biologically active lipid mediators derived from the CYP-dependent metabolism of ω -6 and ω -3 PUFAs regulate an array of cellular responses, including the onset and resolution of acute inflammation. Elevated concentrations of the linoleic acid (LA)-derived epoxyoctadecenoic acids (EpOMEs) have been detected in people with asthma at baseline and following bronchial provocation tests when compared with nonasthmatic controls (Nording et al., 2010; Lundström et al., 2011, 2012; Larsson et al., 2014). Furthermore, elevated concentrations of the EpOMEs and their corresponding dihydrodiols, the dihydroxyoctadecenoic acids (DiHOMEs), have been found in asthmatic and nonasthmatic individuals following exposure to biodiesel exhaust and tobacco smoke, both of which exacerbate asthma (Smith et al., 2005; Nording et al., 2015; Gouveia-Figueira et al., 2017).

Despite well-documented differences in the levels of the CYP-derived oxylipins in individuals with asthma, little is known about the consequences of genetic variants that alter CYP-dependent production of bioactive lipids and the downstream effects on asthma. The objective of this study was to examine the effects of a common allelic variant in the CYP2C8 enzyme (CYP2C8*3; rs11572080 (R139K) and rs10509681(K399R) on asthma symptom control and the production of inflammatory mediators that contribute to asthma exacerbation by lung epithelial cells. Exploring the effects of genetic variation on the metabolism of endogenous substrates by CYPs may increase our understanding of the mechanisms associated with variability in therapeutic responses in children with asthma independent of therapeutic disposition.

Materials and Methods

DNA Sample Collection and Purification. Genomic DNA was collected from saliva samples obtained prospectively from children 2 to 17 years of age with a physician-confirmed diagnosis of asthma. Subjects were recruited from the emergency department and inpatient wards of Primary Children's Hospital in Salt Lake City, Utah. Information about chronic medical conditions, medication use, and chief complaints was collected through a combination of structured interviews and medical chart abstraction. Data were deidentified before genotype analysis. Characteristics of the patient population have been previously described (Stockmann et al., 2013; Deering-Rice et al., 2016; Rapp et al., 2023). Saliva (2 mL) samples were collected using Oragene DNA kits (DNA Genotek Inc., Ottawa, ON, Canada), and genomic DNA was extracted for SNP genotyping following supplier protocols.

Quantification of Asthma Symptom Control. Each patient's level of asthma symptom control was determined at the time of enrollment using a questionnaire based on guidelines from the National Heart Lung and Blood Institute Expert Panel Report 3 (Expert Panel, 2007), as previously described by Stockmann et al. (Stockmann et al., 2013). In this questionnaire, asthma control scores range from 0 (optimal control) to 15 (poor control) as recommended by the American Thoracic Society and European Respiratory Society.

SNP Genotyping. SNP genotyping was performed using custom TaqMan Open Array cards (Life Technologies) at the University of Utah Genomics core facility. Prior to genotyping, 4 ng of genomic DNA was amplified using a custom TaqMan PreAmp MasterMix (Life Technologies). A TaqMan probe-based SNP genotyping assay for CYP2C8*3 (rs11572080) and other CYP and asthma-associated SNPs were contained on the array cards. TaqMan reactions were cycled as recommended by the manufacturer on a Life Technologies QuantStudio 12K instrument. Data clustering analysis and genotype calls were generated using the TaqMan Genotyper software (Life Technologies).

Reagents. LA, 9(10)-EpOME, 12(13)-EpOME, 9(10)-DiHOME, 12(13)-DiHOME, 9(10)-EpOME-d4, 12(13)-EpOME-d4, 9(10)-DiHOME-d4, 12(13)-DiHOME-d4, montelukast, and 12-[[[tricyclo[3.3.1.1.3,7]dec-1-ylamino]carbonyl]amino]-dodecanoic acid (AUDA) were purchased from Cayman Chemical (Ann Arbor, MI). Montelukast 1,2-diol and montelukast-d6 were purchased from Toronto Research Chemicals (North York, ON, Canada). Cigarette smoke condensate (CSC) was prepared from equilibrated 3R4F reference cigarettes (University of Kentucky Reference Cigarette Program, Lexington, KY) using a single-port smoking machine operated essentially as described by the Massachusetts Standard Smoking Regimen but without blocking the vent holes as previously described by Shapiro et al. (Shapiro et al., 2013).

Cell Culture. Cells were maintained in a humidified cell culture incubator at 37°C with a 95% air and 5% CO₂ atmosphere. Human adenocarcinoma cells were purchased from ATCC (Manassas, VA) and cultured in Dulbecco's modified Eagle medium containing 10% fetal bovine serum and 1x penicillin/streptomycin. Human bronchial epithelial cells (BEAS-2B) were purchased from ATCC (Manassas, VA) and cultured in Lechner and LaVeck media (LHC-9). Normal human bronchial epithelial cells immortalized with CDK4 and hTERT (HBEC3-KT) were purchased from ATCC and cultured with airway epithelial cell basal medium supplemented with the bronchial epithelial cell growth kit from ATCC. Primary human small airway epithelial cells (SAEC; donor ID 01925, 00656, 02195, 05100), primary human lung bronchial epithelial cells (donor ID 01344), and primary human bronchial/tracheal epithelial cells (donor ID 00655) were purchased from Lifeline Cell Technology (Frederick, MD) and cultured using the Bronchia Life epithelial airway medium complete kit from Lifeline Cell Technology. All primary cell lines were maintained for no more than five passages according to supplier recommendations.

CYP2C8 Cloning and Site-Directed Mutagenesis. A cDNA clone of the CYP2C8 open reading frame (ORF; GenBank Accession No.: BC020596) was obtained from transOMIC technologies as a bacterial glycerol stock. The CYP2C8 ORF was amplified using Platinum SuperFi PCR Master Mix (Thermo Fisher, Waltham, MA) and oligonucleotides A, 5'-CACCATGGAACCTTT TGTGGTCTCTGGTGC-3' (forward primer) and B, 5'-GACAGGGATGAAG-CAGATCTGGTATGAG-3' (reverse primer). Oligonucleotide A contained the Kozak translation initiation sequence with an ATG initiation codon for proper initiation of translation in mammalian cells and CACC overhang for optimized expression in mammalian cells and directional cloning into the pcDNA3.1 Directional TOPO mammalian expression vector (Thermo Fisher). Oligonucleotide B was designed without a stop codon to fuse CYP2C8 in frame with the C-terminal V5 epitope and 6xHis tag. The polymerase chain reaction (PCR)-amplified product was cloned into the pcDNA3.1 vector according to the manufacturer's instructions and transformed into One Shot TOP10 chemically competent *E. coli* for amplification. Plasmid DNA was isolated using the GenElute HP Plasmid Midiprep Kit (Millipore Sigma), and the insert sequence and orientation was verified by sequencing. Sequencing was performed using the T7 forward and BGH reverse primers in addition to primers beginning at the 429 and 922 of the CYP2C8 ORF. The CYP2C8*3 expression plasmid was created using the Quick-Change II XL Site-Directed Mutagenesis Kit (Agilent Technologies, Santa Clara, CA) according to the manufacturer's instructions using oligonucleotides C, 5'-CGGTCTCAATGCTCTTCTTCCCCATCCCAA-3' (forward primer) and D, 5'-TTGGGATGGGGAAGAAGAGCATTGAGGACCG-3' (reverse primer) for the R139K amino acid mutation and E, 5'-GACTTCCGTGCTACATGATGACAGAGAATTTCCCTAATCCAA-3' (forward primer) and F, 5'-TTGGATT

AGGAAATCTCTGTCATCATGTAGCACGGAAGTC-3' (reverse primer) for the K399R mutation. Recombinant vectors were transformed into XL-10 Gold ultracompetent cells for amplification and the sequences verified as previously described. Finally, both the CYP2C8*1 (reference) and CYP2C8*3 (variant) ORFs were amplified using Platinum SuperFi PCR Master Mix and oligonucleotides A and B and purified using the QIAquick PCR purification kit (Qiagen, Germantown, MD). Following purification, adenosine overhangs were added to the respective PCR products using Taq DNA Polymerase (Thermo Fisher). The products were then cloned into the pcDNA5/FRT/V5-His TOPO TA mammalian expression vector (Thermo Fisher) and the sequence verified before being used to create the CYP2C8*1 and CYP2C8*3 overexpressing BEAS-2B cell lines.

Generation of CYP2C8*1 and CYP2C8*3 Overexpressing Cell Lines. The Flp-In BEAS-2B cell line was created by transfecting BEAS-2B cells with the pFRT/lacZeo vector (Thermo Fisher) and selecting for zeocin resistant cells containing a single integrated FRT site according to the manufacturer's instructions. Briefly, zeocin-resistant foci derived from single cells sorted into wells of a 96-well plate were screened using a TaqMan Copy Number Assay for the lacZ gene (Mr00529369_cn) to identify single integrands. Single integrands were then screened for β -galactosidase activity using ortho-nitrophenyl- β -galactoside, a lactose analog, and chromogenic substrate for β -galactosidase. The colony with the highest β -galactosidase activity was chosen as the host cell line. Human CYP2C8 overexpressing cell lines were created by cotransfecting the Flp-In BEAS-2B host cell line with the pOG44 Flp recombinase expression vector and the pcDNA5/FRT/V5-His TOPO TA expression vectors harboring either CYP2C8*1 or CYP2C8*3 using FuGene6 transfection reagent (Promega, Madison, WI) according to the manufacturer's instructions, with slight modifications. Briefly cells were transfected in a 6-well plate using 5 μ g plasmid DNA per well and a 3:1 FuGene6 to DNA ratio in 250 μ L of Hank's balanced salt solution (Sigma-Aldrich, St. Louis, MO) for 4 hours, after which 2 mL of Dulbecco's modified Eagle medium/F12 medium containing 5% fetal bovine serum was added for an additional 24 hours. After 24 hours, the medium was replaced with LHC-9 and incubated for an additional 48 hours. After 48 hours, cells were cultured in LHC-9 containing hygromycin (20 μ g/mL) until cells in the nontransfected control well were no longer viable. The CYP2C8 overexpressing cell lines were maintained in LHC-9 media containing hygromycin (20 μ g/mL).

mRNA Quantification by Quantitative PCR. Cells were plated at a density of 25,000 to 30,000 cells per cm^2 and cultured for 72 hours prior to treatment. Total RNA was isolated using the PureLink RNA Mini Kit (Invitrogen, Carlsbad, CA), and the concentration and quality of the RNA was determined spectrophotometrically using the NanoDrop One Microvolume UV-Vis Spectrophotometer (Thermo Scientific). cDNA was synthesized from total RNA using the High-Capacity cDNA Reverse Transcription Kit with RNase Inhibitor (Applied Biosystems, Waltham, MA). Quantitative PCR was performed using a Life Technologies QuantStudio 6 Flex instrument and TaqMan probe-based assays for human CYP2C8 (Hs00946140_g1), human CYP2C9 (Hs02383631_s1), human CYP2J2 (Hs00356035_m1), human interleukin 6 (IL-6) (Hs00174131_m1), and human C-X-C motif chemokine ligand 8 (CXCL-8) (Hs00174103_m1). The $\Delta\Delta C_T$ method was used to calculate target gene expression by normalizing to glyceraldehyde 3-phosphate dehydrogenase (Hs02786624_g1) and/or β 2-microglobulin (Hs00187842_m1).

Western Blotting. Cells were plated at a density of 20,000 cells per cm^2 in 6-well plates and cultured for 72 hours. Total protein was harvested on ice using radioimmunoprecipitation buffer, supplemented with 6 M urea, 1% SDS, Halt protease inhibitor (Invitrogen), and ethylenediaminetetraacetic acid. Lysates were sonicated on ice 3x for 3 seconds and clarified by centrifugation at $13,000 \times g$ for 15 minutes at 4°C. Protein concentrations were determined using the bicinchoninic acid method (Thermo Fisher). Twenty-five micrograms of protein were loaded into each well of a 4–12% Bolt Bis-Tris 12-well gel (Invitrogen) and resolved by electrophoresis for 1 hour at 150 V. Protein was transferred to a polyvinylidene fluoride membrane using the iBlot 2 Gel Transfer Device (Life Technologies). After transfer, the membrane was blocked in SuperBlock (Invitrogen) for 1 hour at room temperature. SeeBlue Plus2 prestained protein standard (10 μ L) was used (Invitrogen). A primary rabbit polyclonal antibody against CYP2C8 (PA5-29796; Invitrogen; 1:1000 in 5% bovine serum albumin with 0.1% sodium azide) and a primary rabbit monoclonal antibody against glyceraldehyde 3-phosphate dehydrogenase (2118; Cell Signaling Technology; Danvers, MA; 1:1000 in 5% bovine serum albumin with 0.1% sodium azide) were incubated at 4°C overnight and used in conjunction with horseradish peroxidase-conjugated sheep-anti-rabbit secondary

antibodies (GE Health Sciences, Marlborough, MA; 1:5000 in SuperBlock). Super-Signal West Dura Extended Duration Substrate (Thermo Fisher) was added to the membrane, and immunostaining was visualized using a FluorChem M imager with the chemiluminescence plus markers setting. Bands were quantified using densitometry on ImageJ and normalized to the control cell line.

Lipidomic Analysis. Cell culture media was collected from cells grown to confluence in a 25 cm^2 flask and frozen at -80°C . Nonesterified oxylipins, endocannabinoids, and polyunsaturated fatty acids were isolated from cell culture media using solid phase extraction with 60 mg Hydrophilic-Lipophilic-Balanced columns (Oasis, Waters Corporation, Milford, MA) and quantified by ultra-performance liquid chromatography-tandem mass spectrometry (UPLC-MS/MS) at the West Coast Metabolomics Center at UC-Davis, as previously described (Pedersen and Newman, 2018). Briefly, columns were washed with one column volume of ethyl acetate followed by two column volumes of methanol and further conditioned with two column volumes of 5% methanol, 0.1% acetic acid in water. Next, columns were spiked with 5 μ L butylated hydroxytoluene/ethylenediamine-tetraacetic acid (1:1 methanol: water) and 5 μ L of 250 nM deuterated oxylipin and endocannabinoid surrogates in methanol. Samples (2 mL) were mixed with 1 mL of 5% methanol, 0.1% acetic acid in water, transferred onto the column, and extracted under the gravity. Columns were then washed with 1 column volume of 30% methanol, 0.1% acetic acid in water. Analytical targets were eluted with 0.5 mL methanol followed by 1.5 mL ethyl acetate. Eluents were dried under the vacuum; reconstituted in 50 μ L of 1-cyclohexyl ureido, 3-dodecanoic acid, and 1-phenyl ureido 3-hexanoic acid at 5 μ M in 1:1 methanol: acetonitrile; filtered through 0.1 μ m PVDF spin filter; and collected for mass spectrometry analysis. Residues in extracts were separated on a 2.1 mm \times 150 mm, 1.7 μ m BEH C₁₈ column (Waters) and detected by electrospray ionization with multireaction monitoring on an API 6500 QTRAP (Sciex; Redwood City, CA) and quantified against 7- to 9-point calibration curves of authentic standards using modifications of previously reported methods.

Analysis of Montelukast Metabolism In Vitro. Cells were plated at a density of 20,000 cells per cm^2 in 6-well plates and cultured for 72 hours. Once confluent, cells were incubated with montelukast (1 μ M) for 24 hours and cell culture media was collected for analysis. All incubations were performed in triplicate ($n = 3$). The reaction was terminated by the addition of 500 μ L of ice-cold acetonitrile containing montelukast-d6 (50 ng/mL) as an internal standard. Following the addition of acetonitrile, samples were vortex-mixed and centrifuged at $3350 \times g$ for 5 minutes to remove cellular debris. The supernatant was transferred to a clean culture tube and extracted using 2 mL of methyl-tert-butyl ether. Extracts were vortexed for 30 seconds and centrifuged at $3350 \times g$ for 10 minutes to separate the organic and aqueous phases. The organic layer was collected and dried at 40°C at 15 psi. The residue was reconstituted in 80 μ L of mobile phase (70:30 acetonitrile:0.1% formic acid) and 10 μ L was injected onto the UPLC-MS/MS.

Quantification of Montelukast 1,2-Diol Using UPLC-MS/MS. Concentrations of montelukast and montelukast 1,2-diol were determined using a ThermoScientific Vanquish Flex UPLC System interfaced with an LTQ Velos Pro Linear Ion Trap Mass Spectrometer. Chromatographic separation was achieved using a BEH C₁₈ column (150 \times 3 mm i.d.; 1.7 μ m particle size; Waters) at room temperature. Isocratic elution mode was applied using a mobile phase consisting of acetonitrile and water containing 0.1% formic acid in the proportion of 70/30 (v/v) at a flow rate of 0.25 mL/min. Positive electrospray ionization selective reaction monitoring was used. The MS/MS parameters were optimized by infusion of montelukast and montelukast 1,2-diol into the MS/MS system and the precursor to product ion transitions used were m/z 586.1 \rightarrow 422.0 for montelukast and m/z 602.1 \rightarrow 438.0 for montelukast 1,2-diol. The mass transitions used for the detection of internal standard (montelukast-d6) was m/z 592.1 \rightarrow 428.2. Data acquisition and processing were performed using the Thermo Scientific Xcalibur software. Stock solutions of montelukast and montelukast 1,2-diol were prepared at a concentration of 1.0 mg/mL in methanol and diluted to concentrations between 0.01 and 2.5 μ M and 0.001 and 0.25 μ M, respectively, for use as calibration standards. Montelukast and montelukast 1,2-diol were quantified by using the ratio of peak area of the metabolite to peak area of internal standard. Linear responses ($r^2 > 0.99$) for all analytes were observed over the concentration range evaluated.

Analysis of Linoleic Acid Metabolism In Vitro. Cells were plated at a density of 30,000 cells per cm^2 in 6-well plates and cultured for 96 hours. Once confluent, cells were incubated with linoleic acid (7.5 μ M) in serum-free media for 12 hours. All incubations were performed in triplicate ($n = 3$). Conditioned

cell culture media (1 mL) was collected and subsequently spiked with 9(10)-EpOME-d₄ (0.25 μM), 12(13)-EpOME-d₄ (0.25 μM), 9(10)-DiHOME-d₄ (0.05 μM), and 12(13)-DiHOME-d₄ (0.05 μM) as internal standards. The LA-derived oxylipins were extracted from cell culture media three times using 2 mL ethyl acetate. Extracts were vortexed for 30 seconds and centrifuged at 3350 × g for 5 minutes to separate the organic and aqueous phases. The ethyl acetate layer was collected and pooled in a clean culture tube and dried under nitrogen at 23°C at 15 psi. The residue was reconstituted in 50 μL of methanol and 10 μL was injected onto the UPLC-MS/MS.

Quantification of Oxylipins Using UPLC-MS/MS. Concentrations of oxylipins [LA; 9(10)- and 12(13)-EpOME; 9(10)- and 12(13)-DiHOME] were determined using a ThermoScientific Vanquish Flex UPLC System interfaced with an LTQ Velos Pro Linear Ion Trap Mass Spectrometer. Chromatographic separation was achieved using a BEH C₁₈ column (150 × 3 mm i.d.; 1.7 μm particle size; Waters) at 35°C with gradient elution. Gradient elution was applied using a mobile phase consisting of (1) 0.1% acetic acid in H₂O and (2) 9:1 acetonitrile:isopropanol at a flow rate of 0.25 mL/min. The percentage of B varied as follows: 52.5% B at 0 minute, 52.5%→57.5% (0 to 6 minutes), 62.5% at 6.1 minutes, 62.5%→77% (6.1 to 12.5 minutes), 77%→95% (12.5 to 16 minutes), 95% hold (16 to 19 minutes), 95%→52.5% (19 to 19.1 minutes), and 52.5% hold until 22 minutes. Negative electrospray ionization selective reaction monitoring was used. The MS/MS parameters were optimized by infusion of lipid standard solutions into the MS/MS system, and the precursor to product ion transitions used were *m/z* 279.2→*m/z* 260.2 for linoleic acid, *m/z* 313.2→*m/z* 183.1 for 9(10)-DiHOME, *m/z* 313.2→*m/z* 201.1 for 12(13)-DiHOME, *m/z* 295.2→*m/z* 171.1 for 9(10)-EpOME, and *m/z* 295.2→*m/z* 195.1 for 12(13)-EpOME. The mass transitions used for the detection of internal standards were *m/z* 317.2→*m/z* 185.1 for 9(10)-DiHOME-d₄, *m/z* 317.2→*m/z* 203.1 for 12(13)-DiHOME-d₄, *m/z* 299.2→*m/z* 172.0 for 9(10)-EpOME-d₄, and *m/z* 299.2→*m/z* 198.0 for 12(13)-EpOME-d₄. Data acquisition and processing were performed using Thermo Scientific Xcalibur software. Stock solutions of LA and its derived oxylipins were diluted to concentrations between 2.5 nM and 7.5 μM for use as calibration standards. LA and its derived oxylipins were quantified using the ratio of peak area of the metabolite to peak area of internal standard. LA was quantified using 9(10)-EpOME-d₄ as the internal standard. Linear responses (*r*² > 0.99) for all analytes were observed over the concentration range evaluated.

Statistical Analysis. All experiments were designed to test a preplanned hypothesis, with the exception of studies evaluating the effects of genetic variation on asthma symptom control, which were exploratory in nature. Values are represented as the mean ± S.D. unless stated otherwise. Descriptive statistics for the study population are presented as median and interquartile range for nonnormally distributed variables and numbers and percentages for categorical values. Significance was determined using one or two-way ANOVA with Tukey's post test, unless otherwise stated. A *P* < 0.05 was considered significant.

Results

CYP2C8*3 (rs11572080) Was Associated with Lower Average Asthma Symptom Control Scores. A total of 1693 children with asthma were enrolled in this study. Table 1 shows patient demographics and clinical findings. All patients were screened for polymorphisms in the CYP2C8 gene to evaluate their association with asthma symptom control. The genomic location and minor allele frequency of each polymorphism are shown in Table 2. Notably, the minor allele frequency for rs11572080 was 9.26%, which was comparable to those previously reported in the 1000 Genomes Project [0.83(AFR)–11.83%(EUR)]. The results indicate that allele A of CYP2C8 G-7225 > A (rs11572080; i.e., CYP2C8*3) was associated with lower average asthma control scores (Supplemental Fig. 1). Specifically, mean asthma control scores were 3.69 (*n* = 207) for patients with one or more copies of the CYP2C8*3 allele versus 4.43 (*n* = 965) for the wild-type CYP2C8*1/*1 (G/G) genotype (*P* = 0.0081) (Fig. 1). Homozygosity for the CYP2C8*3 allele was not associated with reduced asthma control scores, presumably due to the limited statistical power associated with an *n* = 10. The effect of the CYP2C8 genotype on asthma control scores was more pronounced among patients with persistent asthma whose treatment regimen included

TABLE 1
Clinical and demographic characteristics of the study population

Characteristics	Patients with asthma n (%)
Number of subjects	1693
Age, median (IQR)	8.46 (6.96)
Sex	
Female	675 (39.85)
Male	1014 (59.85)
Ethnicity	
Hispanic/Latino	324 (19.13)
American Indian/Alaska Native	15 (0.89)
Asian	13 (0.77)
Native Hawaiian/Pacific Islander	47 (2.77)
Black/African American	61 (3.60)
White	1219 (71.96)
Atopic status	
Atopic (documented/diagnosed allergy)	839 (49.53)
Nonatopic	701 (41.38)
Asthma drug categories	
Inhaled corticosteroids	786 (46.40)
Short-acting beta agonists	1428 (84.29)
Long-acting beta agonists	17 (1.00)
Leukotriene modifiers	411 (24.26)
Long-acting muscarinic antagonists	36 (2.13)
Biologic therapy	5 (0.30)

IQR, interquartile range.

an inhaled corticosteroid (fluticasone propionate or beclomethasone propionate) and montelukast (Fig. 2, A and B). When data were stratified by treatment with inhaled corticosteroids, allele A of CYP2C8 G-7225 > A (rs11572080) was associated with lower average asthma control scores: Mean asthma control scores were 3.69 (*n* = 91) versus 5.22 (*n* = 429) for the wild-type CYP2C8*1/*1 (G/G) genotype (*P* = 0.0007) (Fig. 2A). The effects of allele A of CYP2C8 G-7225 > A (rs11572080) were also observed when data were stratified by treatment with montelukast: Mean asthma control scores were 3.63 (*n* = 56) versus 5.34 (*n* = 213) for the wild-type CYP2C8*1/*1 (G/G) genotype (*P* = 0.0237) (Fig. 2B).

The CYP2C8*3 Variant Exhibited Reduced mRNA and Protein Expression in Lung Epithelial Cells. CYP2C8, CYP2C9, and CYP2J2 mRNA are expressed in human lung epithelial cells isolated from the proximal and distal portions of the airways (Supplemental Fig. 2). CYP2C8 mRNA expression was enriched in SAECs isolated from the distal portion of the lung in the 1-mm bronchiole area. Moreover, CYP2C8 mRNA expression was lowest in immortalized bronchial epithelial cells (BEAS-2B and HBEC3-KT). A Flp-In BEAS-2B cell line was used to ensure integration of CYP2C8*1 and CYP2C8*3 at the same specific genomic location. Expression of CYP2C8 mRNA and protein in CYP2C8*1 and CYP2C8*3 overexpressing cell lines was compared using quantitative PCR and Western blot (Fig. 3, A and B). Despite the use of the isogenic host cell line, CYP2C8*3 mRNA (14.2%, *P* = 0.0332) and protein (30.2%; *P* = 0.0031) expression were lower when compared with CYP2C8*1.

CYP2C8*3 Expression Reduced Proinflammatory Signaling by BEAS-2B Cells Treated with CSC. Cells were treated with CSC (89 μg/cm²) for 4 hours (Fig. 4, A and B). No differences were observed in the basal expression of IL-6 or CXCL-8 as a function of CYP2C8 genotype or expression. Treatment of cells transfected with the empty vector with CSC had minimal effect on IL-6 (2.7-fold, *P* = 0.5274) and CXCL-8 (1.4-fold, *P* = 0.9874) mRNA expression. CYP2C8*1 overexpression significantly increased both IL-6 (10.0-fold, *P* < 0.0001) and CXCL-8 (4.1-fold, *P* < 0.0001) mRNA expression induced by CSC. However, increases in IL-6 (2.7-fold, *P* = 0.0077) and CXCL-8 (2.0-fold, *P* = 0.0461) mRNA expression was attenuated with CYP2C8*3 overexpression compared with CYP2C8*1.

TABLE 2
Minor allele frequency for CYP2C8 variants

Allele	SNP_ID	SNP Location	Nucleotide or Amino Acid Change	Minor Allelic Frequency	
				1000 Genome EUR Population	Study Population
CYP2C8*1C	rs17110453	Promoter	T370G	0.138	0.131
CYP2C8*2	rs11572103	Exon 5	Ile269Phe A805T	0.004	0.024
CYP2C8*3	rs11572080	Exon 3	Arg139Lys G416A	0.118	0.093
CYP2C8*4	rs1058930	Exon 5	Ile264Met C792G	0.057	0.073
CYP2C8*5	rs72558196	Exon 3	Thr159 475delA	0	0
CYP2C8*7	rs72558195	Exon 4	Arg186X C556T	0	0
CYP2C8*8	rs72558195	Exon 4	Arg186Gly C556G	0	0
CYP2C8*14	rs188934928	Exon 5	Ala238Pro G712C	0	0.004

CYP2C8*3 Expression Increased the Epoxide-Diol Ratio in Cells Incubated with LA. Comparison of oxylipin profiles in cells overexpressing either CYP2C8*1 or CYP2C8*3 at baseline revealed genotype-dependent differences in the abundance of the esterified and unesterified LA-derived epoxides and dihydrodiols (Supplemental Fig. 3). Specifically, 12(13)-EpOME, 9(10)-DiHOME, and 12(13)-DiHOME were more abundant in CYP2C8*1 overexpressing BEAS-2B cells. Cells were also incubated with LA (7.5 μ M) for 12 hours to assess the effect of CYP2C8 genotype on LA metabolism (Figs. 5 and 6). Representative chromatograms are shown in Supplemental Fig. 4. CYP2C8*1 overexpression reduced (52.2%, $P = 0.0942$) the concentration of LA remaining in cell culture media following the 12-hour incubation period compared with the control cell line (Fig. 5). Compared with CYP2C8*1, CYP2C8*3 was associated with reduced metabolism of LA, as evidenced by higher concentrations of LA (44.2%, $P = 0.2304$) remaining in the cell culture media following the incubation period. This effect was opposite to that observed for montelukast metabolism (Supplemental Fig. 5). Further, treatment with LA increased the concentrations of 9(10)-EpOME, 12(13)-EpOME, and the corresponding dihydrodiols detected in media (Fig. 6, A–D). CYP2C8*3 had no effect on the production of the EpOMEs but was associated with a decrease in the corresponding dihydrodiols when compared with CYP2C8*1. Epoxide to diol ratios were calculated for each cell type (Fig. 6, E and F); CYP2C8*3 was associated

with an increase in the epoxide to diol ratio when compared with CYP2C8*1.

Soluble Epoxide Hydrolase Inhibition Reduced Proinflammatory Signaling by BEAS-2B Cells in Response to CSC. To assess whether genotype-dependent differences in proinflammatory signaling by human bronchial epithelial cells (HBECs) was related to the ratio of the LA-derived oxylipins, cells transfected with the wild-type CYP2C8*1 enzyme were treated with CSC for 4 hours in the presence or absence of AUDA, a soluble epoxide hydrolase (sEH) inhibitor (Fig. 7). AUDA alone reduced IL-6 mRNA expression but had little to no effect on CXCL-8 expression. Treatment with CSC increased IL-6 mRNA expression 10.0-fold ($P < 0.0001$) compared with the vehicle control (Fig. 7A), and cotreatment with AUDA significantly attenuated this effect ($P < 0.0001$). Similar results were observed for CXCL-8 (Fig. 7B).

9(10)-DiHOME Induces Cytokine Expression in HBEC3-KT. To investigate the direct effects of the LA-derived oxylipins on proinflammatory cytokine signaling by HBECs, HBEC3-KT were treated with 9(10)-EpOME, 9(10)-DiHOME, 12(13)-EpOME, or 12(13)-DiHOME (1, 2, or 10 μ M) for 6 hours (Fig. 8). 9(10)-EpOME had no effect on IL-6 or CXCL-8 mRNA expression. However, 9(10)-DiHOME led to a dose-dependent increase in both IL-6 and CXCL-8 mRNA expression. 9(10)-DiHOME (10 μ M) increased IL-6 mRNA expression 14.9-fold ($P < 0.0001$) and CXCL-8 mRNA expression 23.3-fold ($P < 0.0001$) compared with the vehicle control (Fig. 8, A and B). Similarly, 12(13)-EpOME had essentially no effect on IL-6 or CXCL-8 mRNA expression. However, 12(13)-DiHOME led to a dose-dependent increase in both IL-6 and CXCL-8 mRNA expression. 12(13)-DiHOME (10 μ M) increased IL-6 mRNA expression 20.1-fold ($P < 0.0001$) and CXCL-8 mRNA expression 12.3-fold ($P < 0.0001$) compared with the vehicle control (Fig. 8, C and D).

Discussion

Despite the role of CYP-derived mediators in processes central to asthma pathology, the effects of genetic variation on endogenous substrate metabolism in the context of asthma and asthma pharmacotherapy have not been extensively explored. This study identified an association between the CYP2C8*3 variant and improved asthma symptom control among children with persistent asthma. Mechanisms underlying this association were explored in vitro using CYP2C8*1 and CYP2C8*3 overexpressing BEAS-2B cells, and our findings suggest a role for CYP2C8*3-dependent changes in LA metabolism and oxylipin profiles in regulating inflammatory signaling relevant to asthma pathogenesis and pharmacotherapy.

CYP2C8 is primarily responsible for the clearance of montelukast, a CysLTR1 antagonist prescribed for long-term asthma control (Karonen et al., 2012). Cysteinyl leukotrienes (i.e., LTC₄, LTD₄, LTE₄) mediate bronchoconstriction, eosinophil recruitment, mucus secretion, and vascular

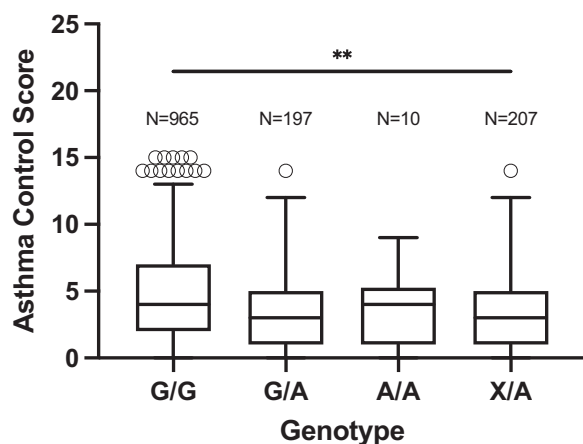


Fig. 1. Comparison of asthma control scores as a function of rs11572080 genotype in a population of children with asthma. Genotype denotes an individual's combination of alleles in the CYP2C8 G-7225 > A (rs11572080) gene polymorphism, where G is the reference allele, A is the variant allele, and X is representative of the presence of either allele. Asthma control scores are scaled from 0 (optimal control) to 15 (poor control). Data are represented as the median and interquartile range (IQR), where the horizontal line indicates the median asthma control score (50th percentile) and the top and bottom of the box is the third quartile (75th percentile) and first quartile (25th percentile), respectively. The whiskers mark the 2.5th and 97.5th percentiles. Data were analyzed for significant differences using the Mann-Whitney U test. $^{**}P < 0.01$.

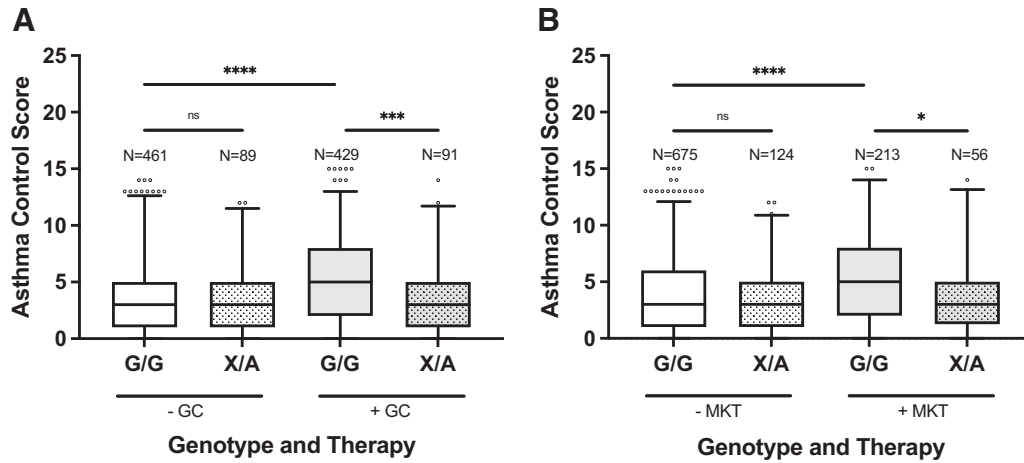


Fig. 2. Comparison of asthma control scores as a function of rs11572080 genotype and treatment with the glucocorticoids (GC) or montelukast (MKT) in a population of children with a confirmed asthma diagnosis. Genotype denotes an individual's combination of alleles in the CYP2C8 G-7225 > A (rs11572080) gene polymorphism, where G is the reference allele, A is the variant allele, and X is representative of the presence of either allele. Asthma control scores are scaled from 0 (optimal control) to 15 (poor control). Data are represented as the median and interquartile range (IQR), where the horizontal line indicates the median asthma control score (50th percentile) and the top and bottom of the box is the third quartile (75th percentile) and first quartile (25th percentile), respectively. The whiskers mark the 2.5th and 97.5th percentiles. Data were analyzed for significant differences using the Kruskal–Wallis *H* test followed by Dunn's post hoc testing to correct for multiple comparisons. **P* < 0.05; ****P* < 0.0005; *****P* < 0.0001.

permeability via the cysteinyl leukotriene receptor 1 receptor (Paggiaro and Bacci, 2011). CYP2C8 also catalyzes the biosynthesis of oxylipins implicated in the pathophysiology of asthma and other airway diseases (Sanak, 2016). Like other CYPs, CYP2C8 exhibits extensive genetic variation, with over 450 variants identified to date (Aquilante et al., 2013). Genetic variants in CYP enzymes involved in endogenous substrate metabolism have been associated with diseases including primary congenital glaucoma (CYP1B1), vitamin D 25-hydroxylase deficiency (CYP2R1), hypertension (CYP4A11, CYP8A1), and coronary heart disease (CYP4A11) (Nebert et al., 2013).

The CYP2C8*3 variant is comprised of the nonsynonymous Arg139Lys (rs11572080) and Lys399Arg (rs10509681) substitutions, which are considered to be in perfect linkage disequilibrium ($r^2 = 1.0$, $P < 0.001$) (Haeggström et al., 2022). According to the 1000 Genome Project, CYP2C8*3 is the most common variant among Europeans (11.83%) and Utah residents with northern and western

European ancestry (13.13%) (Aquilante et al., 2013). The allelic frequency of rs11572080 in this cohort was 9.26%. The beneficial effects of the CYP2C8*3 allele on asthma symptom control were most evident among patients undergoing combination therapy with corticosteroids and montelukast. Previous studies have shown that the CYP2C8*3 increased the metabolic clearance of montelukast in vitro and in vivo (Karonen et al., 2012; Hirvensalo et al., 2018). These findings were replicated here using airway epithelial cells engineered to CYP2C8-overexpressing HBECs. Montelukast administered as monotherapy or in combination with inhaled corticosteroids is shown to improve asthma control, pulmonary function, and overall quality of life in patients with persistent, uncontrolled asthma (Phipatanakul et al., 2003; Bérubé et al., 2014; Esposito et al., 2019; Ikram et al., 2019). As such, results here suggest that the beneficial effects of CYP2C8*3 on asthma symptom control are likely independent of montelukast clearance by CYP2C8.

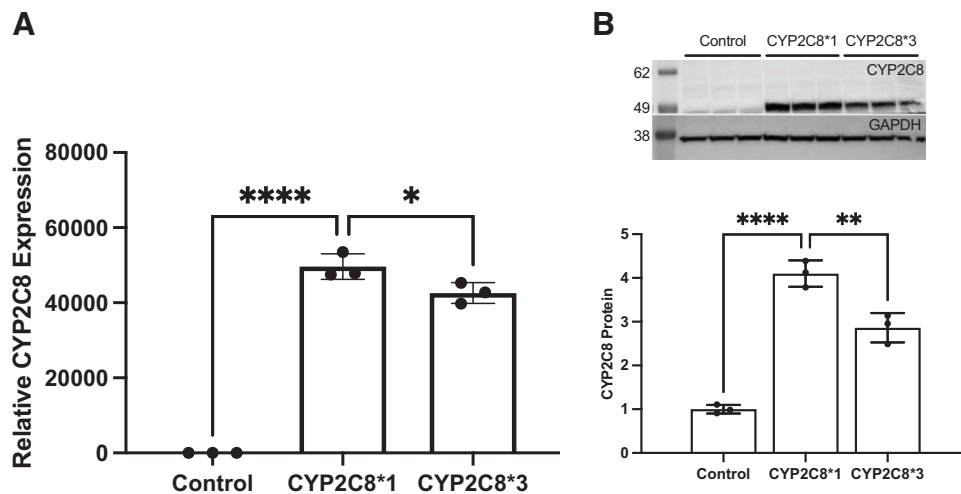


Fig. 3. Relative (A) mRNA and (B) protein expression of CYP2C8 in cells engineered to overexpress CYP2C8*1 and CYP2C8*3. Data were normalized to glyceraldehyde 3-phosphate dehydrogenase expression and are represented as fold change relative to the Flp-In BEAS-2B cell line transfected with the pcDNA5 FRT empty vector. Results are mean ± S.D. (error bars) from $n = 3$ replicates. Data were analyzed for significant differences by one-way ANOVA followed by Tukey post hoc testing to correct for multiple comparisons. **P* < 0.05; ***P* < 0.01; *****P* < 0.0001.

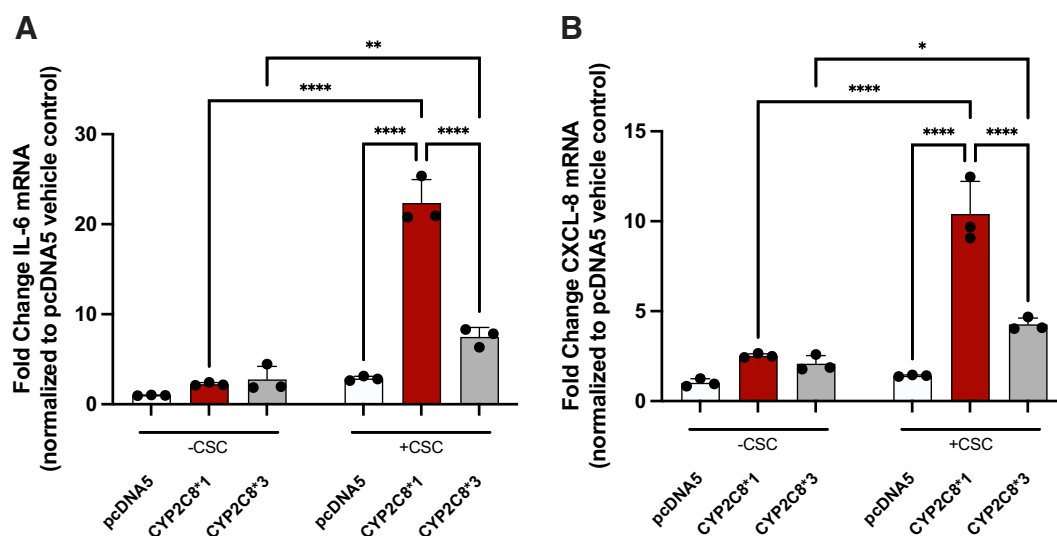


Fig. 4. Effect of the CYP2C8*3 variant on the response of BEAS-2B to CSC ($89 \mu\text{g}/\text{cm}^2$). Relative mRNA expression of (A) IL-6 and (B) CXCL-8 4 hours following exposure to CSC. Data were normalized to glyceraldehyde 3-phosphate dehydrogenase expression and are represented as fold change relative to the pcDNA5 vehicle control. Results are mean \pm S.D. from $n = 3$ replicates. Data were analyzed for significant differences by two-way ANOVA followed by Tukey post hoc testing to correct for multiple comparisons. * $P < 0.05$; ** $P < 0.01$; **** $P < 0.0001$.

CYP2C8 also converts long-chain PUFAs to biologically active epoxides that play important roles in inflammation, angiogenesis, and metabolic regulation (Fleming, 2011; Gilroy et al., 2016; Samokhvalov et al., 2019). CYP2C8 accounts for approximately 7% of total hepatic CYP content but has also been detected in human lung and lung-derived cell lines (Hukkanen et al., 2001; Aquilante et al., 2013). In human lungs, CYP2C8 is expressed by bronchial and bronchiolar epithelial cells, club cells, type II pneumocytes, and alveolar macrophages (Macé et al., 1998; Hukkanen et al., 2001, 2002). Here, CYP2C8 mRNA expression was most abundantly expressed in primary human SAECs, which secrete a variety of proinflammatory mediators in response to oxidative stress and other noxious stimuli (Zhao et al., 2010). Notably, CYP2C8 was expressed at a lower level by CYP2C8*3-overexpressing cells. Reduced protein expression is typically associated with loss-of-function CYP SNPs (Zanger and Schwab, 2013), although the effects of such phenomena are often overlooked unless the resulting phenotype is marked.

Increased sensitivity and reactivity of airway epithelial cells to pharmacological, physical, and chemical stimuli increases the risk of acute asthma exacerbations and increased symptom severity (Hewitt & Lloyd,

2021). Cigarette smoke is a common environmental trigger of asthma and has been linked to accelerated decline in pulmonary function and reduced responsiveness to corticosteroids, presumably due to the neutrophil-dominant (Th1/Th17-dominant) phenotype promoted by exposure (Tiotiu et al., 2021). Overexpression of CYP2C8 in BEAS-2B cells amplified the expression of IL-6 and CXCL-8 in response to CSC treatment compared with the control cell line, where limited induction was observed. However, the response to CSC was attenuated in cells expressing CYP2C8*3 compared with those expressing CYP2C8*1. IL-6 and CXCL-8 released by airway epithelial cells play an important role in asthma pathogenesis via activation and proliferation of immune cells that mediate acute and chronic inflammation (Nakanaga et al., 2007; Rincon and Irvin, 2012). IL-6 is theorized to reflect an activated state of the airway epithelium, a characteristic of AHR associated with allergic sensitization (Neveu et al., 2010). Meanwhile, CXCL-8 elevation has been observed in the sputum and blood of patients with severe asthma and neutrophilia (Lee et al., 2021). It is possible that attenuated expression of IL-6 and CXCL-8 due to CYP2C8*3 expression is relevant in the context of asthma exacerbation and symptom control.

CYP epoxygenases convert LA to the EpOMEs and arachidonic acid (AA) to the epoxyeicosatrienoic acids (EETs) (Bishop-Bailey et al., 2014). The EETs derived from AA have been shown to attenuate cigarette smoke-induced release of CXCL-8 (Ma et al., 2015). A deficiency in the CYP2C8-mediated metabolism of AA to 11(12)- and 14(15)-EET has been reported for CYP2C8*3, although effects on the remaining PUFAs have not been described (Dai et al., 2001). Oxylipin profiling of CYP2C8-overexpressing BEAS-2B cells revealed a change in the levels of 12(13)-EpOME, 9(10)-DiHOME, and 12(13)-DiHOME, but no changes in oxylipins derived from AA. Of the epoxygenated fatty acids, those derived from LA are the most abundant in bronchoalveolar lavage fluid collected from healthy individuals, presumably due to the high abundance of LA in the Western diet (Gouveia-Figueira et al., 2017; Hildreth et al., 2020). Altered levels of 9(10)-EpOME (leukotoxin), 12(13)-EpOME (isoleukotoxin), and the corresponding DiHOMEs have also been associated with acute and chronic inflammatory lung diseases, including acute respiratory distress syndrome (Ozawa et al., 1988), chronic obstructive pulmonary disorder (Balgoma et al., 2016), and allergic asthma (Lundström et al., 2012). Intravenous

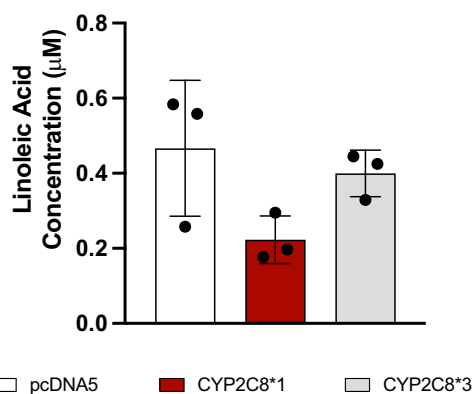


Fig. 5. Metabolism of LA by cells engineered to overexpress CYP2C8*1 and CYP2C8*3. Data are represented as the mean \pm S.D. (error bars) from $n = 3$ replicates. Data were analyzed for significant differences by one-way ANOVA followed by Tukey post hoc testing to correct for multiple comparisons.

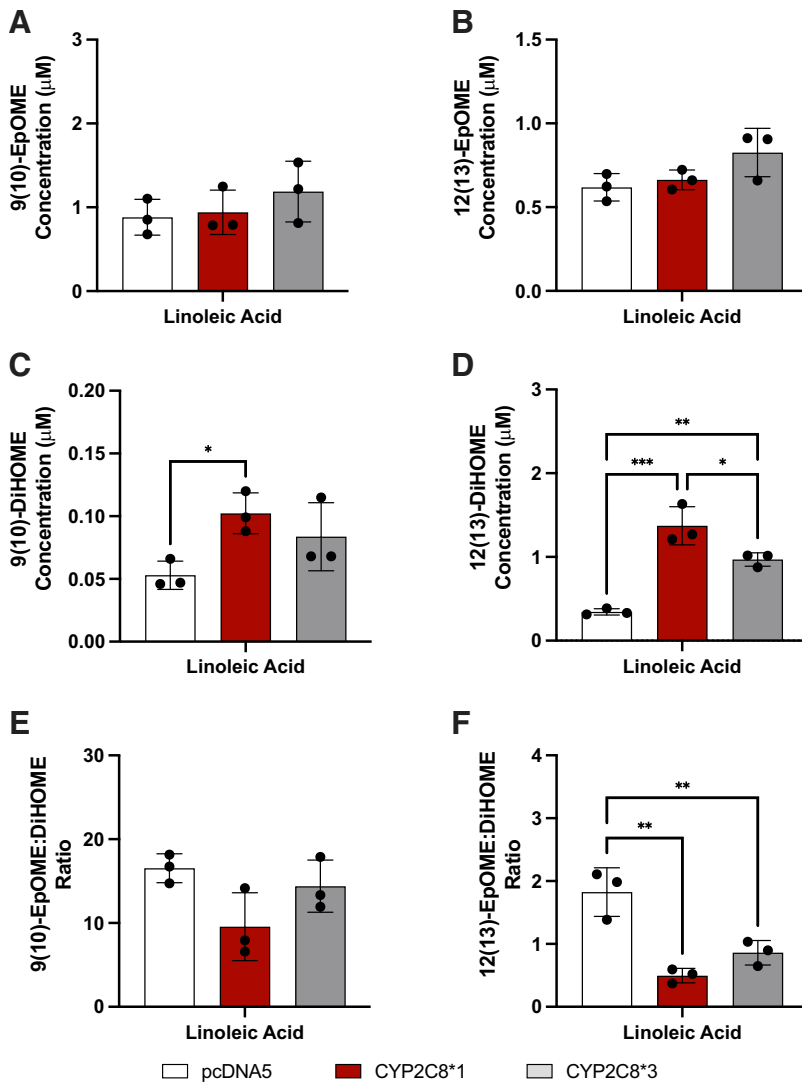


Fig. 6. Formation of the LA-derived epoxides and corresponding diols by cells engineered to overexpress CYP2C8*1 and CYP2C8*3. Data are represented as the mean \pm S.D. (error bars) from $n = 3$ replicates. Data were analyzed for significant differences by one-way ANOVA followed by Tukey post hoc testing to correct for multiple comparisons. * $P < 0.05$; ** $P < 0.01$; *** $P < 0.001$.

administration of 9(10)-EpOME to rats has been shown to promote acute edematous lung injury, an effect ultimately attributed to DiHOME formation (Hu et al., 1988; Zheng et al., 2001). Targeted oxylipin analysis following incubation of BEAS-2B cells with LA revealed an

increase in the LA-derived EpOMEs and DiHOMEs regardless of CYP2C8 genotype. However, CYP2C8 genotype did affect the extent of LA metabolism and the relative abundance of the LA-derived oxylipins, with CYP2C8*3 reducing levels of the linoleate diols

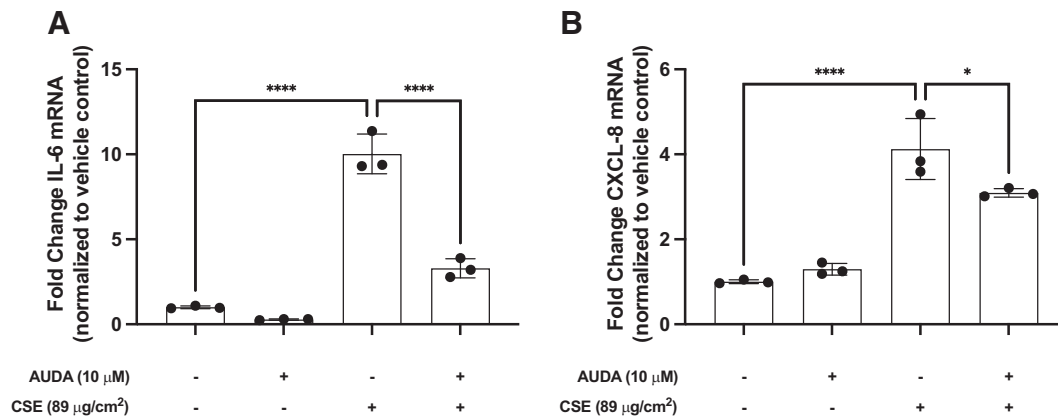


Fig. 7. Effect of sEH inhibition on the response of BEAS-2B to CSC (89 μg/cm²). Relative mRNA expression of (A) IL-6 and (B) CXCL-8 following a 4-hour exposure to cigarette smoke condensate in the presence or absence of AUDA (10 μM). Data were normalized to glyceraldehyde 3-phosphate dehydrogenase expression and are represented as fold change relative to the vehicle control. Results are mean \pm S.D. from $n = 3$ replicates. Data were analyzed for significant differences by one-way ANOVA followed by Tukey post hoc testing to correct for multiple comparisons. * $P < 0.05$; **** $P < 0.0001$.

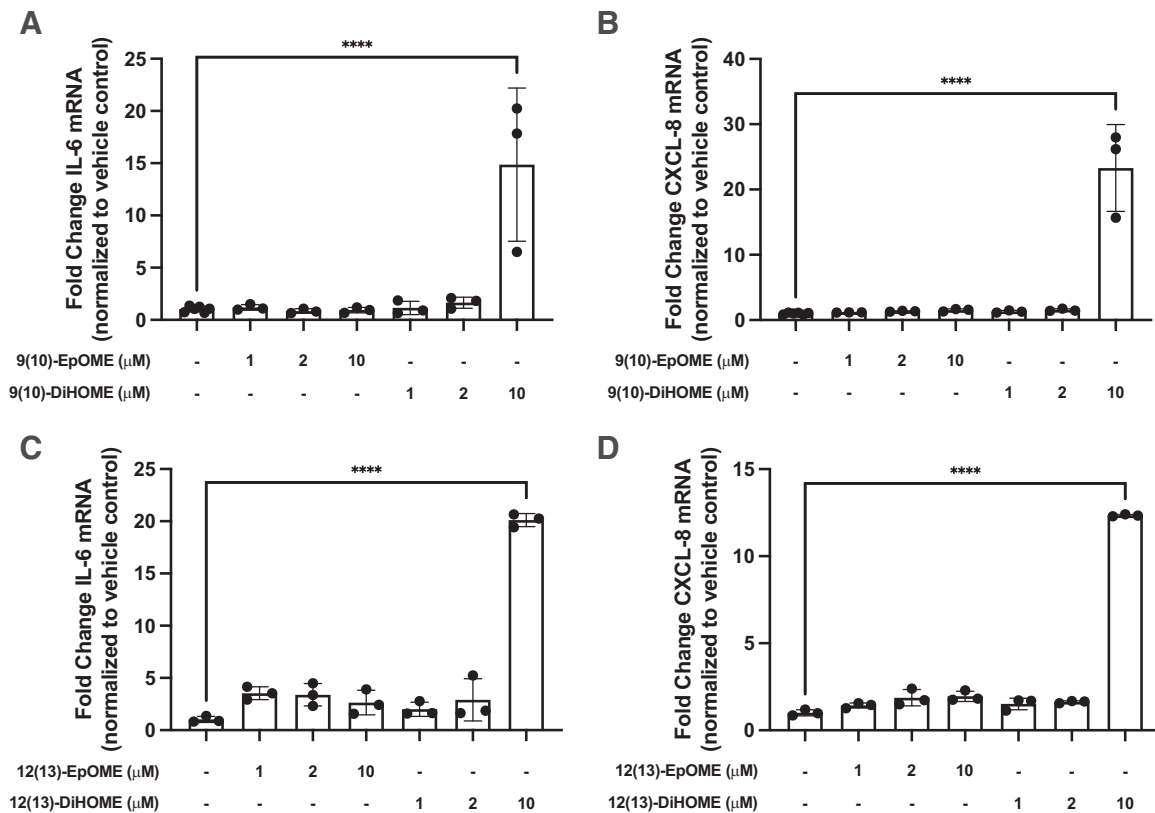


Fig. 8. Effect of 9(10)-EpOME, 9(10)-DiHOME, 12(13)-EpOME, and 12(13)-DiHOME (1, 2, or 10 μ M) on cytokine expression by normal HBEC-3KT. Expression of (A and C) IL-6 and (B and D) CXCL-8 mRNA following treatment with 9(10)-EpOME, 9(10)-DiHOME, 12(13)-EpOME, or 12(13)-DiHOME for 6 hours. Data were normalized to β 2-microglobulin expression and are represented as fold change relative to the vehicle control. Results are mean \pm S.D. from $n = 3$ replicates. Data were analyzed for significant differences by one-way ANOVA followed by Tukey post hoc testing to correct for multiple comparisons. **** $P < 0.0001$.

present in cell culture media following incubation with LA relative to CYP2C8*1.

DiHOMEs activate the mitochondrial permeability transition, resulting in the release of cytochrome c and cell death (Moghaddam et al., 1997; Sisemore et al., 2001). A reduction of cytochrome c oxidase activity in lung mitochondria and the appearance of cytochrome c in the cytosol has been observed with ovalbumin-induced allergic asthma in BALB/c mice (Mabalirajan et al., 2008). Consistent with the association of mitochondrial dysfunction with allergic asthma, peritoneal administration of 12(13)-DiHOME exacerbated lung inflammation in mice sensitized and challenged with cockroach antigen, as evidenced by increased pulmonary leukocyte infiltration and expression of IL-1 α , IL-1 β , and tumor necrosis factor- α (Levan et al., 2019). The same study also found that elevated fecal levels of 12(13)-DiHOME occurred in neonates at risk for childhood asthma and atopy (Levan et al., 2019).

The EpOME to DiHOME ratio is a potential biomarker for disease, including severe COVID-19 (McReynolds et al., 2021). Here, CYP2C8*1 overexpression reduced the EpOME:DiHOME ratio compared with control cells, an effect observed to a lesser extent with CYP2C8*3 overexpression. Inhibition or deletion of sEH, one of two epoxide hydrolases responsible for detoxification of epoxides, reduced cigarette smoke-induced pulmonary inflammation in mice (Smith et al., 2005; Wang et al., 2012; Yang et al., 2015; Liu et al., 2018). Here, cotreatment with AUDA, an sEH inhibitor, reduced the expression of IL-6 and CXCL-8 by HBECs in response to CSC similar to that seen with CYP2C8*3 expression. Further, 9(10)- and 12(13)-DiHOME, but not the precursor epoxides, induced the expression of IL-6 and CXCL-8 by HBECs. Thus, reduced metabolism of LA by CYP2C8*3 and changes in the epoxide to diol ratio may underlie the effects of

CYP2C8*3 on inflammation and asthma, although the mechanism underlying the differences in oxylipin levels requires further study.

To conclude, this study suggests that differential metabolism of LA by airway epithelial cells and likely other cells is the basis for improved asthma symptom control among children with the rs11572080 allele. Specifically, preferential metabolism of LA to the EpOMEs by CYP2C8*3 blunts inflammatory signaling triggered by asthma exacerbating stimuli. Further, the importance of CYP2C8 genotype in relation to apparent differences in the therapeutic efficacy of corticosteroid and montelukast cotherapy may involve preferential inhibition of CYP2C8*1, which could impact EpOME and DiHOME production in a manner that favors greater sensitivity to inflammatory stimuli. As CYP2C8 expression is low in the lung compared with the liver, it is difficult to conclude whether the effects in vivo arise from local or systemic changes in oxylipin levels. Regardless, it is likely that the EpOME:DiHOME ratio plays an important role. Finally, studies in asthmatics have shown that dietary supplementation with ω -3 fatty acids can shift oxylipin profiles toward the production of anti-inflammatory and proresolving lipid mediators (Lundström et al., 2013). It is possible that CYP2C8 genetics may contribute to such effects.

Ethics Approval and Consent to Participate

This study was approved by the University of Utah Institutional Review Board. All participants provided informed consent to participate in this study.

Acknowledgments

The authors acknowledge the DNA/peptide Core of the University of Utah Health Sciences Core for synthesizing and HPLC-purifying primers and probes. The authors would also like to thank John Newman of the US Department of Agriculture, Agricultural Research Service, Western Human Nutrition Research Center Obesity and Metabolism Research Unit for performing the lipidomic analyses presented in this paper.

Data Availability

All data generated or analyzed during this study are included in this published article and can be shared upon request.

Authorship Contributions

Participated in research design: Almestica-Roberts, Reilly.

Conducted experiments: Almestica-Roberts, Nguyen, Sun, Serna, Rapp, Burrell-Gerbers, Memon, Deering-Rice.

Performed data analysis: Almestica-Roberts, Nguyen, Sun, Serna, Rapp, Burrell-Gerbers, Memon, Stone, Nkoy, Rower, Reilly.

Wrote or contributed to the writing of the manuscript: Almestica-Roberts, Nguyen, Memon, Stone, Nkoy, Reilly.

References

- Aquilante CL, Niemi M, Gong L, Altman RB, and Klein TE (2013) PharmGKB summary: very important pharmacogene information for cytochrome P450, family 2, subfamily C, polypeptide 8. *Pharmacogenet Genomics* **23**:721–728.
- Arbitrio M, Scionti F, Di Martino MT, Pensabene L, Tassone P, and Tagliaferri P (2022). Pharmacogenetics/pharmacogenomics of drug-metabolizing enzymes and transporters, in *Comprehensive Pharmacology* (Kenakin T ed) pp 657–697, Elsevier, Amsterdam.
- Balgoma D, Yang M, Sjödin M, Snowden S, Karimi R, Levänen B, Merikallio H, Kaarteenaho R, Palmberg L, Larsson K, et al. (2016) Linoleic acid-derived lipid mediators increase in a female-dominated subphenotype of COPD. *Eur Respir J* **47**:1645–1656.
- Bérubé D, Djangji M, Sampalis JS, and Becker A (2014) Effectiveness of montelukast administered as monotherapy or in combination with inhaled corticosteroid in pediatric patients with uncontrolled asthma: a prospective cohort study. *Allergy Asthma Clin Immunol* **10**:21.
- Bishop-Bailey D, Thomson S, Askari A, Faulkner A, and Wheeler-Jones C (2014) Lipid-metabolizing CYPs in the regulation and dysregulation of metabolism. *Annu Rev Nutr* **34**:261–279.
- Cardoso JdeO, Oliveira RV, Lu JB, and Desta Z (2015) In vitro metabolism of montelukast by cytochrome P450s (CYPs) and UDP-glucuronosyltransferases (UGTs). *Drug Metab Dispos* **43**:1905–1916.
- Cazzola M, Testi R, and Matera MG (2002) Clinical pharmacokinetics of salmeterol. *Clin Pharmacokinet* **41**:19–30.
- Chapman DG and Irvin CG (2015) Mechanisms of airway hyper-responsiveness in asthma: the past, present and yet to come. *Clin Exp Allergy* **45**:706–719.
- Dai D, Zeldin DC, Blaisdell JA, Chanas B, Coulter SJ, Ghanayem BI, and Goldstein JA (2001) Polymorphisms in human CYP2C8 decrease metabolism of the anticancer drug paclitaxel and arachidonic acid. *Pharmacogenetics* **11**:597–607.
- Deering-Rice CE, Stockmann C, Romero EG, Lu Z, Shapiro D, Stone BL, Fassel B, Nkoy F, Uchida DA, Ward RM, et al. (2016) Characterization of transient receptor potential vanilloid-1 (TRPV1) variant activation by coal fly ash particles and associations with altered transient receptor potential ankyrin-1 (TRPA1) expression and asthma. *J Biol Chem* **291**:24866–24879.
- Esposito R, Spaziano G, Giannattasio D, Ferrigno F, Liparulo A, Rossi A, Roviezzo F, Sessa M, Falciami M, Berrino L, et al. (2019) Montelukast improves symptoms and lung function in asthmatic women compared with men. *Front Pharmacol* **10**:1094.
- Expert Panel (2007) Expert Panel Report 3 (EPR-3): guidelines for the diagnosis and management of asthma-summary report 2007. *J Allergy Clin Immunol*, **120**(5 Suppl):S93.
- Fleming I (2011) The cytochrome P450 pathway in angiogenesis and endothelial cell biology. *Cancer Metastasis Rev* **30**:541–555.
- Gilroy DW, Edin ML, De Maeyer RPH, Bystrom J, Newson J, Lih FB, Stables M, Zeldin DC, and Bishop-Bailey D (2016) CYP450-derived oxylipins mediate inflammatory resolution. *Proc Natl Acad Sci USA* **113**:E3240–E3249.
- Gouveia-Figueira S, Karimpour M, Bosson JA, Blomberg A, Unosson J, Pourazar J, Sandström T, Behndig AF, and Nording ML (2017) Mass spectrometry profiling of oxylipins, endocannabinoids, and N-acylthanolamines in human lung lavage fluids reveals responsiveness of prostaglandin E2 and associated lipid metabolites to biodiesel exhaust exposure. *Anal Bioanal Chem* **409**:2967–2980.
- Haegström S, Ingelman-Sundberg M, Pääbo S, and Zeberg H (2022) The clinically relevant CYP2C8*3 and CYP2C9*2 haplotype is inherited from Neandertals. *Pharmacogenomics J* **22**:247–249.
- Hewitt RJ and Lloyd CM (2021) Regulation of immune responses by the airway epithelial cell landscape. *Nat Rev Immunol* **21**:347–362.
- Hildreth K, Kodani SD, Hammock BD, and Zhao L (2020) Cytochrome P450-derived linoleic acid metabolites EpOMes and DiHOMes: a review of recent studies. *J Nutr Biochem* **86**:108484.
- Hirvensalo P, Tornio A, Neuvonen M, Tapaninen T, Paile-Hyvärinen M, Kärjä V, Männistö VT, Pihlajamäki J, Backman JT, and Niemi M (2018) Comprehensive pharmacogenomic study reveals an important role of UGT1A3 in montelukast pharmacokinetics. *Clin Pharmacol Ther* **104**:158–168.
- Hu JN, Taki F, Sugiyama S, Asai J, Izawa Y, Satake T, and Ozawa T (1988) Neutrophil-derived epoxide, 9,10-epoxy-12-octadecenoate, induces pulmonary edema. *Lung* **166**:327–337.
- Hukkanen J, Pelkonen O, Hakkola J, and Raunio H (2002) Expression and regulation of xenobiotic-metabolizing cytochrome P450 (CYP) enzymes in human lung. *Crit Rev Toxicol* **32**:391–411.
- Hukkanen J, Pelkonen O, and Raunio H (2001) Expression of xenobiotic-metabolizing enzymes in human pulmonary tissue: possible role in susceptibility for ILD. *Eur Respir J Suppl* **32**:122s–126s.
- Huo Y and Zhang HY (2018) Genetic mechanisms of asthma and the implications for drug repositioning. *Genes* **9**:237.
- Ikram A, Kumar V, Taimur M, Khan MA, Fareed S, and Barry HD (2019) Role of montelukast in improving quality of life in patients with persistent asthma. *Cureus* **11**:e5046.
- Karonen T, Neuvonen PJ, and Backman JT (2012) CYP2C8 but not CYP3A4 is important in the pharmacokinetics of montelukast. *Br J Clin Pharmacol* **73**:257–267.
- Larsson N, Lundström SL, Pinto R, Rankin G, Karimpour M, Blomberg A, Sandström T, Pourazar J, Trygg J, Behndig AF, et al. (2014) Lipid mediator profiles differ between lung compartments in asthmatic and healthy humans. *Eur Respir J* **43**:453–463.
- Lee Y, Quoc QL, and Park HS (2021) Biomarkers for severe asthma: lessons from longitudinal cohort studies. *Allergy Asthma Immunol Res* **13**:375–389.
- Levan SR, Stammes KA, Lin DL, Panzer AR, Fukui E, McCauley K, Fujimura KE, McKean M, Ownby DR, Zoratti EM, et al. (2019) Elevated faecal 12,13-diHOME concentration in neonates at high risk for asthma is produced by gut bacteria and impedes immune tolerance. *Nat Microbiol* **4**:1851–1861.
- Liu LP, Li B, Shuai TK, Zhu L, and Li YM (2018) Deletion of soluble epoxide hydrolase attenuates mice hyperoxic acute lung injury. *BMC Anesthesiol* **18**:48.
- Lundström SL, Levänen B, Nording M, Klepczynska-Nyström A, Sköld M, Haegström JZ, Grunewald J, Svartengren M, Hammock BD, Larsson BM, et al. (2011) Asthmatics exhibit altered oxylipin profiles compared to healthy individuals after subway air exposure. *PLoS One* **6**:e23864.
- Lundström SL, Yang J, Brannan JD, Haegström JZ, Hammock BD, Nair P, O'Byrne P, Dahlén SE, and Wheelock CE (2013) Lipid mediator serum profiles in asthmatics significantly shift following dietary supplementation with omega-3 fatty acids. *Mol Nutr Food Res* **57**:1378–1389.
- Lundström SL, Yang J, Källberg HJ, Thunberg S, Gafvelin G, Haegström JZ, Grönneberg R, Grunewald J, van Hage M, Hammock BD, et al. (2012) Allergic asthmatics show divergent lipid mediator profiles from healthy controls both at baseline and following birch pollen provocation. *PLoS One* **7**:e33780.
- Ma WJ, Sun YH, Jiang JX, Dong XW, Zhou JY, and Xie QM (2015) Epoxyeicosatrienoic acids attenuate cigarette smoke extract-induced interleukin-8 production in bronchial epithelial cells. *Prostaglandins Leukot Essent Fatty Acids* **94**:13–19.
- Mabalarajan U, Dinda AK, Kumar S, Roshan R, Gupta P, Sharma SK, and Ghosh B (2008) Mitochondrial structural changes and dysfunction are associated with experimental allergic asthma. *J Immunol* **181**:3540–3548.
- Macé K, Bowman ED, Vautravets P, Shields PG, Harris CC, and Pfeifer AMA (1998) Characterization of xenobiotic-metabolizing enzyme expression in human bronchial mucosa and peripheral lung tissues. *Eur J Cancer* **34**:914–920.
- McReynolds CB, Cortes-Puch I, Ravindran R, Khan IH, Hammock BG, Shih PB, Hammock BD, and Yang J (2021) Plasma linoleate diols are potential biomarkers for severe COVID-19 infections. *Front Physiol* **12**:663869.
- Meurs H, Gosens R, and Zaagsma J (2008) Airway hyperresponsiveness in asthma: lessons from in vitro model systems and animal models. *Eur Respir J* **32**:487–502.
- Moghaddam MF, Grant DF, Cheek JM, Greene JF, Williamson KC, and Hammock BD (1997) Bio-oactivation of leukotoxins to their toxic diols by epoxide hydrolase. *Nat Med* **3**:562–566.
- Nakanaga T, Nadel JA, Ueki IF, Koff JL, and Shao MXG (2007) Regulation of interleukin-8 via an airway epithelial signaling cascade. *Am J Physiol Lung Cell Mol Physiol* **292**:L1289–L1296.
- Nebert DW, Wilkval K, and Miller WL (2013) Human cytochromes P450 in health and disease. *Philos Trans R Soc Lond B Biol Sci* **368**:20120431.
- Neveu WA, Allard JL, Raymond DM, Bourassa LM, Burns SM, Bunn JY, Irvin CG, Kaminsky DA, and Rincon M (2010) Elevation of IL-6 in the allergic asthmatic airway is independent of inflammation but associates with loss of central airway function. *Respir Res* **11**:28.
- Nording ML, Yang J, Hegedus CM, Bhushan A, Kenyon NJ, Davis CE, and Hammock BD (2010) Endogenous levels of five fatty acid metabolites in exhaled breath condensate to monitor asthma by high-performance liquid chromatography: electrospray tandem mass spectrometry. *IEEE Sens J* **10**:123–130.
- Nording ML, Yang J, Hoang L, Zamora V, Uyeminami D, Espiritu I, Pinkerton KE, Hammock BD, and Luria A (2015) Bioactive lipid profiling reveals drug target engagement of a soluble epoxide hydrolase inhibitor in a murine model of tobacco smoke exposure. *J Metabolomics* **1**:1.
- Ozawa T, Sugiyama S, Hayakawa M, Satake T, Taki F, Iwata M, and Taki K (1988) Existence of leukotoxin 9,10-epoxy-12-octadecenoate in lung lavages from rats breathing pure oxygen and from patients with the adult respiratory distress syndrome. *Am Rev Respir Dis* **137**:535–540.
- Paggiaro P and Bacci E (2011) Montelukast in asthma: a review of its efficacy and place in therapy. *Ther Adv Chronic Dis* **2**:47–58.
- Pedersen TL and Newman JW (2018) Establishing and performing targeted multi-residue analysis for lipid mediators and fatty acids in small clinical plasma samples. *Methods Mol Biol* **1730**:175–212.
- Phipatanakul W, Greene C, Downes SJ, Cronin B, Eller TJ, Schneider LC, and Irani AM (2003) Montelukast improves asthma control in asthmatic children maintained on inhaled corticosteroids. *Ann Allergy Asthma Immunol* **91**:49–54.
- Rapp E, Lu Z, Sun L, Serna SN, Almestica-Roberts M, Burrell KL, Nguyen ND, Deering-Rice CE, and Reilly CA (2023) Mechanisms and consequences of variable TRPA1 expression by airway epithelial cells: effects of TRPV1 genotype and environmental agonists on cellular responses to pollutants in vitro and asthma. *Environ Health Perspect* **131**:27009.
- Rincon M and Irvin CG (2012) Role of IL-6 in asthma and other inflammatory pulmonary diseases. *Int J Biol Sci* **8**:1281–1290.
- Roberts JK, Moore CD, Ward RM, Yost GS, and Reilly CA (2013) Metabolism of beclomethasone dipropionate by cytochrome P450 3A enzymes. *J Pharmacol Exp Ther* **345**:308–316.
- Samokhvalov V, Jamieson KL, Darwesh AM, Keshavarz-Bahaghighat H, Lee TYT, Edlin M, Lih F, Zeldin DC, and Seubert JM (2019) Deficiency of soluble epoxide hydrolase protects cardiac function impaired by LPS-induced acute inflammation. *Front Pharmacol* **9**:1572.
- Sanak M (2016) Eicosanoid mediators in the airway inflammation of asthmatic patients: what is new? *Allergy Asthma Immunol Res* **8**:481–490.
- Shapiro D, Deering-Rice CE, Romero EG, Hugen RW, Light AR, Veranth JM, and Reilly CA (2013) Activation of transient receptor potential ankyrin-1 (TRPA1) in lung cells by wood smoke particulate material. *Chem Res Toxicol* **26**:750–758.
- Sisemore MF, Zheng J, Yang JC, Thompson DA, Plopper CG, Cortopassi GA, and Hammock BD (2001) Cellular characterization of leukotoxin diol-induced mitochondrial dysfunction. *Arch Biochem Biophys* **392**:32–37.

- Smith KR, Pinkerton KE, Watanabe T, Pedersen TL, Ma SJ, and Hammock BD (2005) Attenuation of tobacco smoke-induced lung inflammation by treatment with a soluble epoxide hydrolase inhibitor. *Proc Natl Acad Sci USA* **102**:2186–2191.
- Stockmann C, Fassl B, Gaedigk R, Nkoy F, Uchida DA, Monson S, Reilly CA, Leeder JS, Yost GS, and Ward RM (2013) Fluticasone propionate pharmacogenetics: CYP3A4*22 polymorphism and pediatric asthma control. *J Pediatr* **162**:1222–1227.
- Stockmann C, Reilly CA, Fassl B, Gaedigk R, Nkoy F, Stone B, Roberts JK, Uchida DA, Leeder JS, Sherwin CMT, et al. (2015) Effect of CYP3A5*3 on asthma control among children treated with inhaled beclomethasone. *J Allergy Clin Immunol* **136**:505–507.
- Tiotiu A, Ioan I, Wirth N, Romero-Fernandez R, and González-Barcala FJ (2021) The impact of tobacco smoking on adult asthma outcomes. *Int J Environ Res Public Health* **18**:992.
- Wang D, Guo Y, Wrighton SA, Cooke GE, and Sadee W (2011) Intronic polymorphism in CYP3A4 affects hepatic expression and response to statin drugs. *Pharmacogenomics J* **11**:274–286.
- Wang L, Yang J, Guo L, Uyeminami D, Dong H, Hammock BD, and Pinkerton KE (2012) Use of a soluble epoxide hydrolase inhibitor in smoke-induced chronic obstructive pulmonary disease. *Am J Respir Cell Mol Biol* **46**:614–622.
- Yang J, Bratt J, Franzi L, Liu JY, Zhang G, Zeki AA, Vogel CFA, Williams K, Dong H, Lin Y, et al. (2015) Soluble epoxide hydrolase inhibitor attenuates inflammation and airway hyperresponsiveness in mice. *Am J Respir Cell Mol Biol* **52**:46–55.
- Zanger UM and Schwab M (2013) Cytochrome P450 enzymes in drug metabolism: regulation of gene expression, enzyme activities, and impact of genetic variation. *Pharmacol Ther* **138**:103–141.
- Zhao CZ, Fang XC, Wang D, Tang FD, and Wang XD (2010) Involvement of type II pneumocytes in the pathogenesis of chronic obstructive pulmonary disease. *Respir Med* **104**:1391–1395.
- Zheng J, Plopper CG, Lakritz J, Storms DH, and Hammock BD (2001) Leukotoxin-diol: a putative toxic mediator involved in acute respiratory distress syndrome. *Am J Respir Cell Mol Biol* **25**:434–438.

Address correspondence to: Dr. Christopher A. Reilly, University of Utah, Department of Pharmacology and Toxicology, 30 S 2000 E, 201 Skaggs Hall, Salt Lake City, UT 84112. E-mail: chris.reilly@pharm.utah.edu
